Title

A Very Long-Acting PARP Inhibitor Suppresses Cancer Cell Growth in DNA Repair-Deficient Tumor Models

Journal

Cancer Research, 81(4)

ISSN

0008-5472

Authors

Fontaine, Shaun D
Ashley, Gary W
Houghton, Peter J
et al.

Publication Date

2021-02-15

DOI

10.1158/0008-5472.can-20-1741

Peer reviewed

Published in final edited form as:

Cancer Res. 2021 February 15; 81(4): 1076–1086. doi:10.1158/0008-5472.CAN-20-1741.

A Very Long-Acting PARP Inhibitor Suppresses Cancer Cell Growth in DNA Repair-Deficient Tumor Models

Shaun D. Fontaine[1], **Gary W. Ashley**[1], **Peter J. Houghton**[2], **Raushan T. Kurmasheva**[2], **Morgan Diolaiti**[3], **Alan Ashworth**[3], **Cody J. Peer**[4], **Ryan Nguyen**[4], **William D. Figg Sr.**[4], **Denis R. Beckford-Vera**[5], **Daniel V. Santi**[1]

[1]ProLynx, San Francisco, California.

[2]Greehey Children's Cancer Research Institute, UT Health San Antonio, Texas.

[3]UCSF Helen Diller Family Comprehensive Cancer Center, San Francisco, California.

[4]Pharmacology Program, Center for Cancer Research, National Cancer Institute, National Institutes of Health, Bethesda, Maryland.

[5]Department of Radiology and Biomedical Imaging, University of California San Francisco, San Francisco, California.

Abstract

PARP inhibitors are approved for treatment of cancers with *BRCA1* or *BRCA2* defects. In this study, we prepared and characterized a very long-acting PARP inhibitor. Synthesis of a macromolecular prodrug of talazoparib (TLZ) was achieved by covalent conjugation to a PEG_{40kDa} carrier via a β -eliminative releasable linker. A single injection of the PEG~TLZ conjugate was as effective as ~30 daily oral doses of TLZ in growth suppression of homologous recombination-defective tumors in mouse xenografts. These included the KT-10 Wilms' tumor with a *PALB2* mutation, the *BRCA1*-deficient MX-1 triple-negative breast cancer, and the

Corresponding Author: Daniel V. Santi, 455 Mission Bay Blvd, Suite 341, San Francisco, CA 94158. Phone: 415-552-5306; daniel.v.santi@prolynxinc.com.

Authors' Contributions

S.D. Fontaine: Conceptualization, resources, formal analysis, supervision, investigation, methodology, project administration, writing—review and editing. **G.W. Ashley:** Conceptualization, formal analysis, supervision, methodology, writing—review and editing. **P.J. Houghton:** Conceptualization, resources, methodology, writing—review and editing. **R.T. Kurmasheva:** Resources, investigation, writing—review and editing. **M. Diolaiti:** Resources, investigation, writing—review and editing. **A. Ashworth:** Conceptualization, resources, supervision, methodology, writing-original draft, project administration, writing—review and editing. **C.J. Peer:** Resources, investigation. **R. Nguyen:** Investigation. **W.D. Figg:** Resources. **D.R. Beckford-Vera:** Investigation. **D.V. Santi:** Conceptualization, resources, supervision, methodology, writing-original draft, project administration, writing—review and editing.

Authors' Disclosures

S.D. Fontaine reports a patent for PCT/US2020/048608 Conjugated Inhibitors of DNA Damage Response pending and reports employment with ProLynx and also holds options to purchase shares in ProLynx. G.W. Ashley reports a patent for PCT/US2020/048608 pending; and reports employment with ProLynx LLC. P.J. Houghton reports other funding from ProLynx outside the submitted work. A. Ashworth reports grants from AstraZeneca; personal fees from Tango Therapeutics, Azkarra Therapeutics, Ovibio Corporation, GenVivo, Genentech; other funding from Tango Therapeutics, Azkarra Therapeutics, Ovibio Corporation, SPARC, Bluestar, Prolynx, Earli, Cura, Gladiator, Circle, Cambridge Science Corporation, and Ambagon outside the submitted work; and has patents on the use of PARP inhibitors held jointly with AstraZeneca, which he has benefitted financially (and may do so in the future). No disclosures were reported by the other authors.

The costs of publication of this article were defrayed in part by the payment of page charges. This article must therefore be hereby marked *advertisement* in accordance with 18 U.S.C. Section 1734 solely to indicate this fact.

Note: Supplementary data for this article are available at Cancer Research Online (http://cancerres.aacrjournals.org/).

BRCA2-deficient DLD-1 colon cancer; the prodrug did not inhibit an isogenic DLD-1 tumor with wild-type *BRCA2*. Although the half-life of PEG~TLZ and released TLZ in the mouse was only ~1 day, the exposure of released TLZ from a single safe, effective dose of the prodrug exceeded that of oral TLZ given daily over one month. μPET/CT imaging showed high uptake and prolonged retention of an 89Zr-labeled surrogate of PEG~TLZ in the MX-1 *BRCA1*-deficient tumor. These data suggest that the long-lasting antitumor effect of the prodrug is due to a combination of its long $t_{1/2}$, the high exposure of TLZ released from the prodrug, increased tumor sensitivity upon continued exposure, and tumor accumulation. Using pharmacokinetic parameters of TLZ in humans, we designed a long-acting PEG~TLZ for humans that may be superior in efficacy to daily oral TLZ and would be useful for treatment of PARP inhibitor-sensitive cancers in which oral medications are not tolerated.

Significance: These findings demonstrate that a single injection of a long-acting prodrug of the PARP inhibitor talazoparib in murine xenografts provides tumor suppression equivalent to a month of daily dosing of talazoparib.

Introduction

PARP is a key coordinator of the DNA damage response (DDR). The PARP enzymes bind to single-strand breaks (SSB) of damaged DNA, catalyze transfer of ADP-ribose to target proteins to recruit DNA repair factors, and reseal SSBs in base excision repair and in topoisomerase (Top1) cleavage complexes (1, 2). SSBs that escape repair can form double-strand breaks that require homologous recombination repair (HRR) to avoid cell death. Hence, cells with defective HRR—arising from deficiencies in repair proteins such as *BRCA1/2* and others (3, 4)—are reliant on PARP and may be targeted with PARP inhibitors (PARPi) to cause synthetic lethality. Thus, PARPi are an important class of therapeutic agents that target cancers with defective DDR and increase tumor sensitivity to agents causing DNA damage (5, 6).

From 2014 to present, four PARPi have been approved for every day or twice a day oral use in treatment of human cancers (Fig. 1A; ref. 4). There is compelling evidence that continuous PARP inhibition is more beneficial than intermittent inhibition (7, 8). However, as with any frequently dosed drug, the daily administered PARPi exhibit high C_{max} values and high peak-to-trough excursions of drug concentration. Thus, it is reasonable to believe that the prolonged exposure and lower C_{max} and C_{max}/C_{min} that could be afforded by a very long-acting PARPi might provide a more effective, less toxic therapeutic.

Several putative slow-releasing liposomal nanoparticles of encapsulated talazoparib (9, 10) and olaparib (11, 12) have been studied as potential delivery systems for PARPi. The liposomal PARPi showed tumor growth inhibition and increased survival in mouse xenografts compared with controls and daily free PARPi. However, the relatively short $t_{1/2}$ of such formulations required one to three injections per week to achieve beneficial effects. As a result, to date, long-acting formulations of PARPi have not yet achieved their potential as chemotherapeutic agents.

We have developed a general approach for half-life extension of therapeutics in which a drug is covalently tethered to a long-lived carrier by a linker that slowly cleaves by β-elimination

to release the drug (Fig. 1B; ref. 13). The cleavage rate is determined by the nature of an electron-withdrawing "modulator" (Mod) that controls the acidity of the adjacent C–H bond, and is unaffected by enzymes or general acid/base catalysts. A carrier used for β-eliminative linkers is often a long-lived circulating macromolecule—such as high molecular weight polyethylene glycol (PEG; ref. 13). For this purpose, 4-arm PEG_{40kDa}—a 15-nm-diameter nanocarrier—may be optimal because smaller PEGs have shorter half-lives, whereas larger PEGs all show similar elimination rates. The prodrug is usually eliminated with a $t_{1/2}$ similar to that for carrier, and the apparent $t_{1/2}$ of the released drug is usually similar to the $t_{1/2}$ of the conjugate.

There are constraints that make certain small molecules more or less addressable by the β-eliminative half-life extension technology. First, there are limitations on the amount of prodrug that can be administered, so the released drug must be sufficiently potent to maintain target engagement over the desired duration. Likewise, the V_d of the free drug cannot be so high that wide distribution exceeds the amount the prodrug can supply. Second, while the $t_{1/2}$ of the released drug is a function of the linker used, the blood levels of the released drug are directly related to the $t_{1/2}$ of the free drug; a free drug with a longer $t_{1/2}$ reduces the amount needed to achieve a particular level. Finally, the drug needs to possess a functional group suitable for attachment of a β-eliminative linker, which thus far includes primary and secondary amines, hydroxyl/phenolic, or sulfhydryl groups (13–16).

Previously, we studied the β-eliminative PEG_{40kDa}~SN-38 conjugates PLX038 and PLX038A (14, 17)—the former of which is in clinical trials (NCT02646852; https://clinicaltrials.gov/). The conjugates release SN-38—the active metabolite of irinotecan—which stabilizes the Top1-DNA cleavage complex and inhibits DNA strand ligation. As amechanism-based DNA damaging agent,the drug targets the DDR and synthetic lethality in tumors. The favorable properties of these prodrugs are (i) a long $t_{1/2}$ approximating the 6-day $t_{1/2}$ for renal elimination of the PEG_{40kDa} carrier in humans—with concomitant benefits of low C_{max} and prolonged exposure—and (ii) high accumulation and retention in tumors (18). The latter occurs because of the long circulating $t_{1/2}$ and near-ideal size and shape of the ~15-nm-diameter nanocarriers to penetrate large pores of tumor vasculature. Because these propitious properties emanate from the PEG_{40kDa} nanocarrier and not the drug, we posited they should be conferrable to other drugs as well—such as a PARPi.

In choosing a PARPi to demonstrate the utility of the β-eliminative technology platform, talazoparib appeared as an attractive choice. Although PARP catalytic activity is inhibited comparably by the various PARPi, talazoparib (TLZ) is ~100-fold more potent at trapping PARP-DNA complexes and much more potent as an antitumor agent (1, 19–21). Indeed, TLZ requires only 1 mg/day dosing in adults (22) compared with hundreds of mg/day for other PARPis, and the C_{max} of TLZ in humans is ~15- to 50-fold lower than that of other PARPi.

At the outset of this work, it was unclear whether we could connect a β-eliminative linker to TLZ and, if so, whether the attachment would be sufficiently stable to support drug release over long periods. When feasible, the linker–drug conjugates of Fig. 1A are easily prepared as carbamates by reaction of a basic amine group of a drug with an activated

carbonate of the linker (13). However, many small-molecule drugs—including TLZ—do not have nucleophilic amines and require an adaptation of the technology whereby the linkers are modified for attachment to poorly nucleophilic heteroatoms (Fig. 1C; refs. 14, 15) — such as the phthalazinone moiety of TLZ. Here, the revised linkers contain a methylene adaptor that connects the carbamate nitrogen to the heteroatom of the drug (X-Drug), and an electron-withdrawing N-substituent (R_1) that suppresses spontaneous S_N1 cleavage of the adaptor–drug heteroatom bond. Upon β-elimination a carbamic acid is released, which rapidly loses CO_2 to form a Mannich base intermediate that disassembles to form CH_2O, a primary amine and the free drug.

In this work, we developed novel chemistry that enables attachment of β-eliminative linkers to TLZ to form long-acting PEG~TLZ prodrugs, characterized several such conjugates and determined the pharmacokinetics and antitumor activity of one of them. We report that a single injection of the PEG_{40kDa}~TLZ provides durable, long-lasting antitumor effects in HRR-defective mouse xenografts persisting a month or more. We posit explanations for the remarkable effects of this prodrug. Finally, we modeled the pharmacokinetics of PEG~TLZ conjugates in humans, and propose a prodrug that could be dosed every two weeks to continuously maintain TLZ at a concentration within its known therapeutic window.

Materials and Methods

Detailed descriptions of materials and procedures used for syntheses, pharmacokinetic studies, and tumor xenograft experiments are presented in the Supplementary Information.

Materials

PEG_{40kDa}-$[NH_2]_4$ was purchased from NOF America (Sunbright PTE-400PA) and TLZ was from ApexBio or MedKoo. Other purchased chemicals were of the highest purity available from commercial sources, and used without further purification.

Chemistry

Synthesis of linkers, connection of linkers to TLZ or olaparib, and coupling of linker–PARPi conjugates to PEG followed general approaches (17), and full details of syntheses are provided in the Supplementary Information. The identity and purity of entities were verified by HPLC and, where appropriate, NMR and LC/MS. Synthesis of PEG_{40kDa}~$(TLZ)_3$DFB and chelation to ^{89}Zr used a slight modification of the method described for the related PEG_{40kDa}~$(SN\text{-}38)_3$DFB conjugate (18).

In vitro drug release kinetics

Solutions of PEGylated conjugates at pH 1.1 to 9.4 were kept at 37°C in an HPLC autosampler. At appropriate intervals, aliquots were injected on a C18 HPLC column and eluted with gradient of H_2O and MeCN containing 0.1% TFA. Peak areas measured by UV-Vis were normalized against an internal standard and data was fitted to a single-phase exponential equation to determine reaction rates of linker cleavage.

Pharmacokinetic studies

Male CD-1 mice (4–6 weeks old) were dosed intravenously or intraperitoneally with solutions of PEG~TLZ. For studies with stable PEG~TLZ, mice ($N = 4$) were dosed and 40 μL blood samples were obtained at appropriate times by serial micro-sampling via tail-snip (23) performed at Charles River Laboratories; samples were immediately acidified and stabilized with 0.1 vol pH 4.5 buffer (14), and centrifuged to provide plasma samples which were frozen at −80°C until analysis. For studies with releasable PEG~TLZ, larger groups of mice ($N = 20$) were dosed and composite sampling was performed in which blood obtained at sequential time points were taken from different animals ($n = 4$), providing sufficient volume for analyses of both PEG~TLZ and free TLZ; as before, blood samples were rapidly acidified with pH 4.5 buffer, and centrifuged to provide plasma samples which were kept frozen at −80°C until analysis.

For analysis of PEG~TLZ, 10 μL plasma was treated with 50 μL MeOH/0.5% AcOH. After vortexing and centrifugation, samples were diluted with 200 μL of H_2O/0.5% AcOH, injected onto a C18 HPLC column, and eluted with a gradient of H_2O and MeCN containing 0.1% TFA. PEG~TLZ concentrations were determined by interpolation of peak areas of a standard curve and plotted versus time. The LLOQ for PEG~TLZ was 16 pmol in 10 μL serum.

Free TLZ in acidic plasma samples was isolated by solid-phase extraction and measured by UHPLC/MS-MS using a modification of a reported procedure (24). Briefly, chromatographic separation was achieved using an Acquity BEH C18 column by gradient elution with 0.1% HCO_2H in H_2O and CH_3CN as the mobile phase; an AB Sciex QTRAP 5500 mass spectrometer was used to monitor transitions of talazoparib (*m/z* 381.1284.7) and [^{13}C, $^{2}H_4$]-TLZ (*m/z* 386.4286.3) using multiple reaction monitoring (MRM) in the positive ion mode. Results were linear over the range of 0.50 to 100 ng/mL TLZ, with excellent accuracy (<3.7%) and correlation to predicted values ($r^2 = 0.998$; Supplementary Tables S1 and S2). The method was reproducible with between-run and within-run precision in the ranges of 2.0% to 9.1% and 1.9% to 8.7%, respectively.

Antitumor activity of PEG_{40kDa}~$(TLZ)_4$ in murine xenografts

Animal studies were carried out in accordance with UCSF and UT Institutional Animal Care and Use Committees. All cell lines were authenticated via STR and tested negative for mycoplasma prior to use. The KT-10 Wilms tumor was established directly from patient tissue grafted into CB17 scid$^{-/-}$ mice as reported previously (25), and had not been in culture, and were used tumor on passage 22.TC-71 cells were obtained from the Children's Caner Repository, Children's Oncology group, established as a xenograft in CB17 *scid*$^{-/-}$ female mice (25) from a Master Bank of STR authenticated lines that are mycoplasma-free, and used within 6 months of being established in culture at passage 8. MX-1 cells were obtained from the NCI and xenografts were established in female NCr nude mice as reported (17, 26) and used on *in vivo* passage 3. DLD-1 *BRCA2*$^{WT/WT}$ and *BRCA2*$^{-/-}$ cells were obtained from Horizon Discovery and were established in female NCr nude mice by subcutaneous implantation of 5×10^6 cells in 1:1 SFM:Matrigel in the flank in a manner

analogous to previously reported methods (27) at an unknown passage number but were authenticated by STR and myco tested a week prior to implantation.

When tumors reached ~300 mm^3 (MX-1, TC-71, DLD-1) or ~600 mm^3 (KT-10) mice received a single intraperitoneal dose of 4 to 40 μmol/kg of PEG_{40kDa}~$(TLZ)_4$ or every day oral gavages of free TLZ (0.4 μmol/kg/day; ref. 8). Tumor volumes measured by caliper [0.5 × (length × $width^2$)] and body weights were determined twice weekly. Event-free survival analyses were performed using Prism 8.0 with an event defined as a two-fold increase in tumor volume from the day of treatment.

Tumor uptake of PEG_{40kDa}~$(TLZ)_3$^{89}Zr

Mice (N = 4/group) bearing ~80 mm^3 MX-1 xenografts were injected with 7 nmol (~145 mCi), of the stable ^{89}Zr-labeled prodrug surrogate via the tail vein. μPET/CT scans were acquired at intervals from at 2- to 528-hour postinjection. μPET/CT scans, image analysis and data modeling were performed as reported previously (18).

Results

Chemistry

Connection of a β-eliminative linker to a drug requires a nucleophilic site on the drug for attachment. The 2-NH of the phthalazinone moiety of TLZ has a calculated pK_a of 12.1 using MoKa (28), which is in excellent agreement with the pK_a of 11.9 we determined by spectrophotometric titration at 310 nm (see below); MoKa did not predict the pK_a of the N7 aromatic NH of TLZ, which is beyond the upper limit of ~13 the software can calculate. Also, aromatic NH groups that are much less basic than the predicted pK_b of N7 of TLZ (pK_b = −0.85) have pK_a values >17 (29). Hence, we surmised that treatment of TLZ with a strong base would preferentially ionize the phthalazinone NH of TLZ to its conjugate base and activate the 2-N position towards alkylation.

First, we prepared a permanent $mPEG_{20kDa}$~TLZ conjugate **3A** to determine the stability of the attachment chemistry (Fig.2). Treatment of TLZ with NaHMDS followed by the O-azidohexyl N-aryl-N-chloromethylcarbamate **1A** gave a product with the expected mass of the N_3-linker~TLZ **2A.** Then, **2A** was attached to $mPEG_{20kDa}$-dibenzocyclooctyne (DBCO) by strain-promoted alkyne-azide cyclo-addition (SPAAC) to afford the $mPEG_{20kDa}$~TLZ conjugate **3A.** The conjugate showed no detectable release of TLZ at pH 5.0 to 9.4 for 15 hours at 37°C, demonstrating stability of the linker attachment to TLZ (Supplementary Fig. S1A).

We next repeated the synthetic sequence using N-chloromethyl carbamate **1B** bearing a -SO_2Me modulator to provide the releasable mPEG~TLZ conjugate **3B** (Fig. 2). Unlike the stable conjugate **3A,** at pH 7 to 9 there was a hydroxide-catalyzed cleavage of **3B** with k_{OH} = 9.1 ± 0.75 $M^{-1}sec^{-1}$ and an extrapolated $t_{1/2}$ of ~80 hours at pH 7.4. However, an intermediate formed concomitantly with conjugate disappearance and showed a long $t_{1/2}$ for conversion to TLZ of ~12 hours (Supplementary Figs. S1B and S1C). The intermediate was identified as the N-arylamino-TLZ Mannich base by mass spectrometry and by UV-VIS spectrum characteristics showing of conjoined TLZ (λ_{max} = 310 and 350 nm) and aryl

amine (λ_{max} = 260) moieties (Fig. 1C; Supplementary Figs. S2A–S2C). Because the $t_{1/2}$ of the intermediate was longer than the elimination $t_{1/2}$ of TLZ, we were concerned that *in vivo* clearance of an accumulated intermediate might compromise the pharmacokinetics of TLZ. To mitigate this risk, we sought to modify the linker to increase the rate of collapse of the Mannich intermediate.

It has been shown that strong electron withdrawing groups at the N-substituent stabilize a Mannich base (15, 30). To promote breakdown of the intermediate, we reduced the electron withdrawing ability of the N-substituent by changing the N-aryl group to a methoxyethyl moiety. Stable N_3-linker-TLZ conjugates **2C** and releasable **2D** bearing N-methoxylethyl groups were prepared from the appropriate N-methoxyethyl-N-chloromethyl carbamates **1C,D** and TLZ (Fig. 2).

Next, mPEG$_{20kDa}$~TLZ conjugates **3C** and **3D** were prepared from **2C** and **2D,** respectively, and mPEG$_{20kDa}$-DBCO as above by SPAAC. Conjugate **3C** was stable at pH 5.0 to 9.4 at 37°C for over 1 week (Supplementary Fig. S3A). In contrast, TLZ was released from conjugate **3D** over pH 7.4to 9.4with k_{OH} = 5.1 ±0.80$M^{-1}s^{-1}$, or $t_{1/2}$ at pH 7.4 of ~150 hours (Supplementary Fig. S3B). Unlike the analogous N-aryl carbamate **3B,** a Mannich intermediate could not be detected by HPLC during release of TLZ.

For *in vivo* studies, we prepared analogous stable and releasable 4-arm PEG$_{40kDa}$~(TLZ)$_4$ conjugates, **4C** and **4D** (Fig. 3). These conjugates have a four-fold higher drug capacity than 3 and a polymer size optimized to retard renal elimination (13). PEG$_{40kDa}$~(TLZ)$_4$ **4D** was prepared in 65% yield by SPAAC reaction of N_3-linker~TLZ **2D** with PEG$_{40kDa}$tetra-5-hydroxylcyclooctyne [PEG$_{40kDa}$(5HCO)$_4$]. The conjugate showed excellent stability at pH 1 and 5 with >95% remaining after 1 month at 37°C. At higher pH, TLZ was released in a hydroxide-catalyzed reaction with k_{OH} = 4.8 $M^{-1}s^{-1}$ between pH 7.4 and 9.4 and $t_{1/2}$ of 160 hours at pH 7.4 (Fig. 4A). During yield optimization of **2D,** we observed formation of variable amounts of a N-7 hydroxy methylated linker~TLZ byproduct, likely emanating from the presence of formaldehyde during alkylation of TLZ by the linker. However, we found the byproduct could be converted to **2D** by treatment with acidic ethylene glycol or its formation could be completely suppressed by quenching the alkylation reaction with aqueous Tris pH 7.5 at −78°C.

Linker **2C** was used to unambiguously assign the position of attachment of the linker to TLZ at N2 by 2D NMR (COSY, HSQC, and HMBC; Supplementary Figs. S4–S6). In addition, spectrophotometric titration of TLZ at pH 9 to 13 shows an increase in absorbance at 310 and confirms a pK_a of 11.9 (Supplementary Figs. S7A and S7B). However, no corresponding spectral change characteristic of the ionization of the phthalazinone was observed for PEG~TLZ **4C** (Supplementary Figs. S7C and S7D) supporting the structural assignment of linker **2C**. Finally, the linker could be coupled to olaparib (below), which has only a single NH at the phthalazinone that could serve as the alkylation site.

Finally, olaparib—which contains only a single potentially ionizable NH at the phthalazinone moiety—was alkylated with *N*-methoxyethyl-*N*-chloromethyl carbamates **1C** and **1D** containing either a stable or releasable linker, respectively, via the approach used

for TLZ. The N_3-linker~olaparib intermediates were then PEGylated by reactions with $mPEG_{20kDa}$-DBCO. Permanently linked olaparib was completely stable for 1 week at pH 7.4 and 9.6, 37°C (Supplementary Fig. S8A). In contrast, the olaparib conjugate with a β-eliminative linker released the drug with extrapolated $t_{1/2}$ 235 hours at pH 7.4, 37°C, close to that of the analogous TLZ conjugate **3D** (Supplementary Fig. S8B).

Pharmacokinetics of PEG_{40kDa}~$(TLZ)_4$ 4D in the mouse

In this work, we administered PEG_{40kDa}~$(TLZ)_4$ by intraperitoneally rather than more conventional intravenous administration of such macromolecular conjugates. However, once in the central compartment the pharmacokinetics of intraperitoneally- and intravenously-administered conjugates were essentially identical (Supplementary Fig. S9).

Figure 4B shows the *C* versus *t* plots for intraperitoneally-administered 4D and the TLZ released from **4D,** and Table 1 provides pharmacokinetic parameters calculated from these data. After a short absorption phase, $t_{1/2,\alpha}$ ~1.8 hours, **4C**and **4D** reach identical C_{max} values in the central compartment and then diverge in concentrations as TLZ is released from **4D** (Supplementary Fig. S9; Supplementary Table S3). We have previously shown that the pharmacokinetics of a circulating releasable prodrug and the released drug is described by $k_\beta = k_1 + k_3$ (13), where k_β is the observed elimination rate, k_1 is the rate of linker cleavage, and k_3 is the elimination rate of the prodrug. A $t_{1/2,3}$ of 23 hours is obtained as the kb of the stable conjugate **4C.** From this, and the $t_{1/2,\beta}$ of 21 hours for **4D,** the *in vivo* linker cleavage $t_{1/2,1}$ was determined as ~200 hours, consistent with the *in vitro* cleavage $t_{1/2}$ of 160 hours at pH 7.4. The TLZ released from **4D** has a $t_{1/2,\beta}$ of 32 hours, and represents ~3% of the concurrent concentration of the prodrug (a replicate experiment of **4D** is reported in Supplementary Fig. S10 and Supplementary Table S4).

Employing the reported pharmacokinetic parameters of TLZ in mice (31), we calculated C_{max} values of ~200 nmol/L for every day and twice a day oral doses of TLZ used to treat mouse xenografts (32), and about 270 nmol/L for the MTD of 0.25 mg (0.66 μmol/kg) twice a day in tumor-free mice (32). The C_{max} of TLZ released from PEG_{40kDa}~$(TLZ)_4$ is ~26-fold higher than the MTD of twice a day oral TLZ. With a $t_{1/2}$ for TLZ released from PEG_{40kDa}~$(TLZ)_4$ of 32 hours, the concentration from a single effective dose of 30 μmol/kg PEG_{40kDa}~$(TLZ)_4$ exceeds C_{max} or MTD concentrations of oral TLZ for 5 to 6 days yet shows no toxic effects. Moreover, the AUC_{Wk} of TLZ released from **4D** is 30- to 40-fold higher than that of every day oral TLZ and, remarkably, the AUC_{Wk} is 18-fold higher than the MTD of oral TLZ. Hence, mice are much more tolerant to TLZ slowly released from **4D** than to every day or twice a day oral dosing of free TLZ.

In vivo evaluation of PEG_{40kDa}~$(TLZ)_4$

The HR-deficient KT-10 Wilms tumor PDX with a *PALB2* mutation is highly sensitive to TLZ (32, 33). Daily oral doses of 0.17 to 0.33 mg (0.43 to 0.87 μmol)/kg TLZ over 4 weeks produced complete responses (CR) that were maintained for a 12-week study period (33). Cohorts of mice ($n = 5$) bearing subcutaneous KT-10 tumors were treated with a single intraperitoneal injection of PEG_{40kDa}~$(TLZ)_4$ **4D** at 5 to 40 μmol/kg of (Fig. 5).[1] Tumor volumes were measured weekly, and event-free survival (EFS) was calculated for

each group, where the event was defined as doubling of the initial tumor volume on the first day of treatment (25). Dosing **4D** at 40 μmol/kg caused an average ~17% weight loss at day 7, but all animals recovered by day 14. The dose-dependent tumor growth responses and Kaplan–Meier event-free survival distributions of **4D** are shown in Fig. 5A and B; control tumors had a median EFS of 4 days. With **4D** at 5 μmol/kg TLZ, three tumors showed slight regressions and the median EFS was 17 days with all tumors reaching the event. At 10 μmol/kg, all tumors regressed >50% and showed a median EFS of 41 days with 4/5 tumors reaching an event. At higher doses of **4D** at 20 and 40 μmol/kg, all tumors showed EFS >8 weeks; there was complete regression with regrowth of four of five tumors in the group treated with 20 μmol/kg and two of five tumors in mice treated with 40 μmol/kg. The EFS T/C for a dose of **4D** at 10 μmol/kg was 9.3, which qualifies it as a highly active agent against this tumor (25).

Next, we treated mice bearing TLZ-sensitive *BRCA1*-deficient MX-1 tumors (8, 34) with every day oral TLZ and single intraperitoneal injections of PEG_{40kDa}~$(TLZ)_4$ **4D** (Fig. 5C and D). Control tumors had a median 2×-EFS of 7 days and with 0.4 μmol/kg TLZ there was growth suppression for ~3 weeks, after which, tumors grew and reached median EFS at 35 days (Fig. 5D). Clearly, the MX-1 tumor is not as sensitive to TLZ as KT-10, which shows maintained CRs over 12 weeks with only 0.1 mg/kg TLZ every day dosing (33). With **4D** at 40 μmol/kg TLZ, animals lost ~9% weight by day 8 and 2 of 5 died. The remaining 3 mice regained their initial weight and did not show tumor outgrowth after as long as 50 days; the censored deceased mice did not allow reliable EFS analysis. Mice tolerated single doses of **4D** at 5 to 30 μmol/kg without weight loss. A dose of **4D** at 13 μmol/kg resulted in a median EFS of 31 days, which was similar to the 35-day EFS for free TLZ at 0.4 μmol (0.15 mg)/kg/day. The EFS T/C of 4.4 for **4D** at 13 μmol/kg indicates the drug is highly active at this low dose (25). Notably, when tumors in six control mice grew to ~1,200 mm^3, treatment with a single injection of **4D** at 30 μmol/kg resulted in almost complete regression of tumors in the surviving 2 of 6 mice by 3 weeks (Supplementary Fig. S11A). The antitumor effects of PEG_{40kDa}~$(TLZ)_4$ **4D** were a consequence of the TLZ released from the prodrug since a single dose of the stable PEG_{40kDa}~$(TLZ)_4$ **4C** at 30 μmol/kg showed no tumor growth inhibition (Supplementary Fig. S11B). Also, effects of **4D** on MX-1 tumor growth dose either intraperitoneally or intravenously were indistinguishable (Supplementary Fig. S12). Thus, the relevant effects of PEG_{40kDa}~$(TLZ)_4$ are the same whether administered intraperitoneally or intravenously.

We also examined the Ewing sarcoma TC-71 tumor, which is relatively resistant to daily treatment with oral TLZ and shows low EFS activity (33). As expected, tumor growth was not inhibited by **4D** concentrations as high as 40 μmol/kg, and the EFS curves indicate insignificant activity (Fig. 5E and F). Thus, a tumor which is not affected by frequently administered oral TLZ is neither affected by the long acting PEG_{40kDa}~$(TLZ)_4$ **4D.**

Finally, we treated an isogenic pair of DLD-1 $BRCA^{-/-}$ and DLD-1 $BRCA2^{wt/wt}$ with daily oral TLZ at 0.87 μmol/kg (0.33 mg/kg) or single intraperitoneal injection of PEG~TLZ.

[1]Each molecule of 4-arm PEG40kDa~(TLZ)4 conjugates contains four equivalents of TLZ but doses are reported as μmol TLZ in the conjugate. For example, a dose of 40 μmol **4D** contains 40 μmol of TLZ.

In the *BRCA2*$^{-/-}$ tumor, one injection of PEG~TLZ **4D** at 20 μmol/kg is equi-effective in suppressing tumor growth as 21 daily doses of 0.87 μmol (0.33 mg)/kg/day (Fig. 5G). Median EFS was increased six-fold for animals treated with **4D** at 10 μmol/kg and 11- or 13-fold for animals treated with daily TLZ × 21 days or a single dose of 20 μmol/kg **4D,** respectively (Fig. 5H). In contrast, the *BRCA2* replete DLD-1 tumor is resistant to either QD oral TLZ or IP PEG~TLZ (Fig. 5I and J); here, there is no increase in median EFS of treated animals versus controls.

Tumor uptake and pharmacokinetics of PEG_{40kDa}~$(TLZ)_3$$^{89}Zr$

As described for PEG_{40kDa}~$(SN\text{-}38)_3$$^{89}Zr$ (18), we prepared a surrogate of the stable **4C** that contained TLZ on three arms of four-arm PEG_{40kDa} and ^{89}Zr on the other. Uptake and associated kinetic parameters of the ^{89}Zr-labeled nanocarriers were determined in the MX-1 tumor and normal mouse tissues using μPET/CT imaging (Supplementary Fig. S13; Supplementary Table S5) as described previously (18).The time-activity curves for normal tissues showed high levels at early times due to perfused blood which, with exception of liver, was followed by monophasic loss to background levels; in liver, the radioactivity plateaued at about ~10% of the initial dose. In tumors, levels were initially low but increased to ~10% of initial dose over several days and was eliminated with a very long $t_{1/2}$ of ~17 days.

Pharmacokinetic modeling of PEG_{40kDa}~$(TLZ)_4$ in the human

We previously described approaches for modeling the pharmacokinetics of drugs released from a prodrug by β-eliminative linkers (13, 17). To estimate the $t_{1/2,\beta}$ of the circulating prodrug and the released drug, one needs to assign the rate of linker cleavage, k_1, the rate of elimination of the prodrug, k_3, and the pharmacokinetics of the free drug in the species of interest. The elimination $t_{1/2,3}$ of PEG_{40kDa} in humans is ~6 days (35) and, as with PLX038, a PEG_{40kDa}~$(TLZ)_4$ prodrug with *in vivo* cleavage $t_{1/2,1}$ of ~12 days in humans should provide TLZ with a $t_{1/2,\beta}$ ~4 days. We used the pharmacokinetic parameters of free TLZ in humans (22), and assumed that continuous exposure of PARP between the10 nmol/L C_{min} and the 55 nmol/L C_{max}—the therapeutic window—is required for efficacy. Perhaps coincidentally, the 10 nmol/L C_{min} of TLZ in the human is essentially the same as the 12 nmol/L C_{min} of the most effective 0.165 mg/kg ever day dose of TLZ in mice (8). Simulations show that every 2 weeks administration of PEG_{40kDa}~$(TLZ)_4$ prodrug containing 50 mg TLZ to humans would give a steady state concentration of TLZ that is always above C_{min} and within the efficacy/tolerability boundaries defined withdaily1 mg TLZ (Fig. 6). It should be possible to increase the dose of Q2Wk PEG_{40kDa}~$(TLZ)_4$ 1.7-fold and still maintain TLZ within the presumed therapeutic window which would increase tumor exposure and could increase efficacy.

Discussion

The objective of this work was to develop a long-acting prodrug of TLZ that benefits from improved pharmacokinetics and pharmacology. The specific aims were to (i) develop chemistry that enables attachment of TLZ to long-lived carriers via β-eliminative linkers, (ii) determine the pharmacokinetics of PEG~TLZ in mice, (iii) ascertain its antitumor activity

in mouse xenografts, and (iv) design a PEG~TLZ prodrug with pharmacokinetics optimized for human use.

We first developed chemistry that allows attachment of linkers to TLZ. The drug has a phthalazinone moiety with a pK_a of ~12 at the 2-NH, which we targeted as a potential attachment site. We first coupled the conjugate base of TLZ with N-aryl-N-chloromethyl carbamates to provide both stable and β-eliminative releasable azido–linker–TLZ conjugates. After attachment to mPEG$_{20kDa}$, the conjugate with the permanent linker was stable at pH 5 to 9.4, whereas that with the Mod = MeSO$_2$- β-eliminative linker released TLZ with a $t_{1/2}$ of ~80 hours at pH 7.4. However, a relatively stable N-arylamino Mannich base intermediate formed during TLZ release due to the high pK_a of the leaving group and low pK_a of the N-substituent (15, 30).

To avoid possible consequences of an accumulated intermediate, we prepared a linker containing a weaker electron withdrawing N-carbamate substituent—methoxyethyl—which was predicted to promote rapid collapse of the Mannich base intermediate (15, 30). We attached a stable linker containing a N-methoxyethyl carbamate to TLZ and unambiguously showed it resided at N2. We then prepared the releasable mPEG$_{20kDa}$~TLZ conjugate with a N-methoxyethyl carbamate and MeSO$_2$- modulator. TLZ was released with a $t_{1/2}$ of ~160 hours at pH 7.4 but, in contrast to the analogous N-aryl carbamate, no intermediate was detected during drug release. Finally, we prepared the analogous 4-arm PEG$_{40kDa}$~(TLZ)$_4$ conjugate **4D** to optimize the drug capacity and renal elimination rate of the conjugate for anticipated *in vivo* studies.

The $t_{1/2,\beta}$ of PEG$_{40kDa}$~(TLZ)$_4$ in the mouse was ~20 hours and the $t_{1/2,\beta}$ of the released TLZ showed a $t_{1/2}$ of ~30 hours. Remarkably, the TLZ released from a single, safe, and effective dose of 30 μmol/kg of the prodrug gave a C_{max} that exceeded the C_{max} for the MTD of twice every day oral TLZ by about 30-fold, and remains above the MTD C_{max} of oral TLZ for ~5 days. Likewise, the AUC of the released TLZ from a single effective dose of the prodrug was ~30- to 40-fold higher than efficacious daily or twice every day oral TLZ over 1 week, and showed ~20-fold higher weekly AUC than that for twice a day oral TLZ at its MTD. These results clearly show that mice are much more tolerant to TLZ slowly released from PEG$_{40kDa}$~(TLZ)$_4$ than to every day or twice a day oral dosing of free TLZ.

It has recently been proposed (36) that the ratio of the average steady state concentration (C_{ss}) to *in vitro* cell potency (IC$_{50}$) of anticancer agents can be used to guide dosing in humans. Here, some 25 therapies showed a median C_{SS}/IC$_{50}$ of 1.2, indicating a relatively narrow therapeutic window where higher doses are not tolerated, and lower doses result in insufficient target engagement. However, drugs that have a high C_{ss}/IC$_{50}$ can be administered at higher doses, and lower doses may provide similar efficacy with a more favorable toxicity profile. Every day oral TLZ showed a C_{SS}/IC$_{50}$ of 1, indicating a narrow therapeutic window; however, with a C_{SS}/IC$_{50}$ of ~30 to 40, the TLZ released from PEG~TLZ achieves a much higher C_{SS}. Hence, we posit that the exposure of TLZ released from the prodrug could be substantially increased over the C_{ss} of daily oral TLZ to achieve increased efficacy without increased toxicity.

We tested the antitumor effects of the PEG_{40kDa}~$(TLZ)_4$ against TLZ-resistant and HRR-defective TLZ-sensitive mouse xenografts. As expected, the TLZ-resistant Ewing sarcoma TC-71 tumor (33) was unresponsive toward the TLZ prodrug. In contrast, KT-10, a HRR-defective, TLZ-sensitive Wilms tumor PDX with a frameshift mutation in *PALB2* (33), MX-1, a *BRCA1*-deficient TNBC (8, 34) and DLD-1 $BRCA2^{-/-}$, a *BRCA2*-deficient colon cancer, were highly sensitive to every day oral TLZ or a single injection of PEG_{40kDa}~$(TLZ)_4$. In contrast to DLD-1 $BRCA2^{-/-}$, DLD-1 $BRCA2^{wt/wt}$, an isogenic BRCA2-replete tumor, was completely resistant to both every day TLZ and single dose PEG~TLZ. Hence, HRR-defective tumor lines—epitomized by tumors deficient in *BRCA1/2*—are highly sensitive to single dose PEG_{40kDa}~$(TLZ)_4$.

Although the $t_{1/2,\beta}$ of PEG_{40kDa}~$(TLZ)_4$ is 1 day and the $t_{1/2,\beta}$ of free TLZ is only 3 hours in the mouse (31), a single nontoxic dose of the prodrug suppressed growth of susceptible tumors for 1 month or more and, in many cases, resulted in maintained complete responses. The long-acting antitumor effects of PEG_{40kDa}~$(TLZ)_4$ were clearly due to the released TLZ, since the stable surrogate of the TLZ prodrug, 4C, showed no activity. In general, the amount of TLZ in a single efficacious dose of the PEG_{40kDa}~$(TLZ)_4$ conjugate was equivalent to the same amount of free TLZ administered in divided daily doses for 4 or more weeks. Although we did not investigate multidose scheduling, the data suggest that administration of PEG_{40kDa}~$(TLZ)_4$ once every month should be sufficient to suppress tumor growth for extended periods.

We pondered why the antitumor effects of a single injection of PEG_{40kDa}~$(TLZ)_4$ in PARPi-sensitive mouse xenografts are so long lasting. First, the very high concentrations over prolonged periods achieved by the released TLZ should have profound antitumor effects—much greater than daily free TLZ. Second, tumor cells may become significantly more sensitive to a drug as a function of the time of exposure (37, 38) and, indeed, the inhibitory potency of TLZ towards chronic lymphocytic leukemia increases after a short pretreatment with the drug (39); the lower drug concentration requirements of a sensitized tumor could counter the reduced TLZ concentration that occurs over time. Finally, the large prodrug accumulates and is retained in tumors, slowly releasing its cargo in the tumor environment over long periods. Indeed, as observed with an analogous prodrug of SN-38 (18), the surrogate stable PEG_{40kDa}~$(TLZ)_3{}^{89}Zr$ conjugate has a high accumulation of 10% of the initial dose/mL in the MX-1 xenograft, and very long efflux $t_{1/2}$ of 17 days.

Using the pharmacokinetic parameters for TLZ in humans (22), and approaches for pharmacokinetic modeling of circulating macromolecular prodrugs (17), we simulated the pharmacokinetics of PEG_{40kDa}~$(TLZ)_4$ conjugates in humans. Importantly, PEG_{40kDa} prodrugs have a much longer lifetime in humans than mice because the renal elimination of the prodrug is much longer—$t_{1/2}$ ~6 days versus <1 day, respectively. We estimated that Q2Wk dosing of appropriate amounts of a PEG_{40kDa}~$(TLZ)_4$ prodrug having an *in vivo* release $t_{1/2,1}$ of 12 days could maintain TLZ within its known therapeutic window and cause the needed continuous inhibition of PARP. Moreover, if—as in the mouse—the TLZ released from PEG_{40kDa}~$(TLZ)_4$ is more tolerable than daily TLZ, it should be possible to achieve higher levels of TLZ with concomitant higher tumor exposure and consequent higher efficacy. An EPR effect of the prodrug—as observed in mouse tumors with such

nanocarrier conjugates—should not be essential for its efficacy in the human but, if present, would provide additional therapeutic benefits of passive tumor targeting. Hence, we posit that every 2 weeks dose of a properly designed intravenously-administered PEG_{40kDa}~$(TLZ)_4$ would be at least as efficacious and possibly superior to daily oral TLZ in humans.

If tumor accumulation and retention of PEG_{40kDa}~$(TLZ)_4$ in a human tumor occurs to the extent it does in the mouse MX-1 xenograft, the effects could provide additional advantages to the prodrug. For example, the EPR effect helps surmount PARPi-resistance in HRR-deficient mouse tumors that overexpress drug efflux transporter P-glycoprotein (40). In the same model, a releasable PEG~SN-38 akin to PEG_{40kDa}~$(TLZ)_4$ overcomes drug efflux by concentrating in the tumor and causing a high drug concentration gradient opposing drug efflux (41). Another benefit of a tumor-targeted PARPi prodrug with a long tumor efflux $t_{1/2}$ might be the avoidance of toxicities of combinations with a DNA damaging agent using a “gapped-schedule” approach (42). Here, the tumor would be first loaded via EPR with the long-acting PEG_{40kDa}~$(TLZ)_4$, which is then allowed to clear from normal tissue; then, the DNA damaging agent would administered within a time window when the PEG_{40kDa}~$(TLZ)_4$ is retained in the tumor but not normal tissue. The gapped-schedule ensures that when the DNA-damaging agent is introduced, the tumor remains loaded with the PARPi while normal tissue including bone marrow has been cleared of the inhibitor and hence less susceptible to toxicities of the combination.

An intravenously-administered long-acting PEG_{40kDa}~$(TLZ)_4$ could offer an important therapeutic option in patients with PARPi-sensitive tumors for whom every day oral drug administration may be impractical, intolerable, or less effective—as exemplified by the following. (i) Orally administered PARPi may not be tolerable in patients with gastric, pancreatic, or hepatic cancer who have had surgical procedures and experience malabsorption or dumping syndrome. (ii) Functional bowel obstruction in the setting of peritoneal carcinomatosis following metastasis of pancreatic, ovarian, stomach, or colon cancers may not allow oral absorption of drugs. (iii) Patients with head and neck squamous cell carcinoma with esophageal strictures may not be able to swallow oral medications. (iv) PARPi themselves and drug combinations—in particular, with DNA damaging agents—can cause significant nausea and vomiting leading to a risk of missing doses of an oral PARPi. (v) Finally, an intravenously-administered PEG-PARPi prodrug might provide higher exposure of certain tumors to the released drug than frequent oral administration of the free PARPi. For example, in addition to systemic treatment of a *BRCA1/2* deficient primary breast tumor, PEG_{40kDa}~$(TLZ)_4$ is the ideal size nanomedicine to accumulate in early-stage brain metastasis (43), where it could serve as a slow releasing reservoir of the PARPi. Supporting this is the observation that NKTR-102—a PEG_{20kDa}~CPT-11 prodrug similar to PEG_{40kDa}~$(TLZ)_4$—accumulates in brain metastases from breast cancer and slowly releases CPT-11 in the tumor microenvironment (44). Thus, in certain situations an intravenously-administered PARPi prodrug could have significant benefits over an orally administered PARPi.

In summary, we have developed a novel method of conjugating linkers to the phthalazinone moiety of PARPi inhibitors such as TLZ and olaparib. We prepared a PEG_{40kDa}~$(TLZ)_4$ prodrug that provides TLZ with a long *in vivo* $t_{1/2,\beta}$ of ~30 hours and extremely

high exposure in the mouse—far surpassing those achievable with daily oral TLZ. In mouse xenografts of tumors with defective HRR, a single nontoxic dose of PEG_{40kDa}~$(TLZ)_4$ suppresses tumor growth for about one month, and is equi-effective to daily administration of TLZ over that period. We suggest that the long-lasting effect is due to the long $t_{1/2}$ of PEG_{40kDa}~$(TLZ)_4$, the remarkably high exposure of TLZ released from the prodrug, increased sensitivity of the tumor upon continued drug exposure, and/or tumor accumulation of the macromolecular prodrug with local drug release. Finally, using known pharmacokinetic parameters of TLZ in humans, we designed a long-acting PEG~TLZ for human therapeutics that may be superior to daily oral TLZ, and would be useful for treatment of PARPi-sensitive cancers in which oral medications are poorly tolerated.

Supplementary Material

Refer to Web version on PubMed Central for supplementary material.

References

1. Murai J, Huang SY, Das BB, Renaud A, Zhang Y, Doroshow JH, et al. Trapping of PARP1 and PARP2 by clinical PARP inhibitors. Cancer Res 2012;72:5588–99. [PubMed: 23118055]
2. Murai J, Huang SY, Renaud A, Zhang Y, Ji J, Takeda S, et al. Stereospecific PARP trapping by BMN 673 and comparison with olaparib and rucaparib. Mol Cancer Ther 2014;13:433–43. [PubMed: 24356813]
3. Lord CJ, Ashworth A. BRCAness revisited. Nat Rev Cancer 2016;16:110–20. [PubMed: 26775620]
4. Lord CJ, Ashworth A. PARP inhibitors: synthetic lethality in the clinic. Science 2017;355:1152–8. [PubMed: 28302823]
5. Drean A, Lord CJ, Ashworth A. PARP inhibitor combination therapy. Crit Rev Oncol Hematol 2016;108:73–85. [PubMed: 27931843]
6. Stewart RA, Pilie PG, Yap TA. Development of PARP and immune-checkpoint inhibitor combinations. Cancer Res 2018;78:6717–25. [PubMed: 30498083]
7. Drew Y, Ledermann J, Hall G, Rea D, Glasspool R, Highley M, et al. Phase 2 multicentre trial investigating intermittent and continuous dosing schedules of the poly(ADP-ribose) polymerase inhibitor rucaparib in germline BRCA mutation carriers with advanced ovarian and breast cancer. Br J Cancer 2016; 114:723–30. [PubMed: 27002934]
8. Shen Y, Rehman FL, Feng Y, Boshuizen J, Bajrami I, Elliott R, et al. BMN 673, a novel and highly potent PARP1/2 inhibitor for the treatment of human cancers with DNA repair deficiency. Clin Cancer Res 2013;19:5003–15. [PubMed: 23881923]
9. Zhang D, Baldwin P, Leal AS, Carapellucci S, Sridhar S, Liby KT. A nanoliposome formulation of the PARP inhibitor Talazoparib enhances treatment efficacy and modulates immune cell populations in mammary tumors of BRCA-deficient mice. Theranostics 2019;9:6224–38. [PubMed: 31534547]
10. Baldwin P, Likhotvorik R, Baig N, Cropper J, Carlson R, Kurmasheva R, et al. Nanoformulation of talazoparib increases maximum tolerated doses in combination with temozolomide for treatment of ewing sarcoma. Front Oncol 2019;9:1416. [PubMed: 31921673]
11. van de Ven AL, Tangutoori S, Baldwin P, Qiao J, Gharagouzloo C, Seitzer N, et al. Nanoformulation of olaparib amplifies PARP inhibition and sensitizes PTEN/TP53-deficient prostate cancer to radiation. Mol Cancer Ther 2017;16: 1279–89. [PubMed: 28500233]
12. Mensah LB, Morton SW, Li J, Xiao H, Quadir MA, Elias KM, et al. Layer-by-layer nanoparticles for novel delivery of cisplatin and PARP inhibitors for platinum-based drug resistance therapy in ovarian cancer. Bioeng Transl Med 2019;4: e10131.
13. Santi DV, Schneider EL, Reid R, Robinson L, Ashley GW. Predictable and tunable half-life extension of therapeutic agents by controlled chemical release from macromolecular conjugates. Proc Natl Acad Sci U S A 2012;109:6211–6. [PubMed: 22474378]

14. Santi DV, Schneider EL, Ashley GW. Macromolecular prodrug that provides the irinotecan (CPT-11) active-metabolite SN-38 with ultralong half-life, low C (max), and low glucuronide formation. J Med Chem 2014;57:2303–14. [PubMed: 24494988]
15. Schneider EL, Robinson L, Reid R, Ashley GW, Santi DV. beta-Eliminative releasable linkers adapted for bioconjugation of macromolecules to phenols. Bioconjug Chem 2013;24:1990–7. [PubMed: 24171387]
16. Ashley G, Santi DV; Prolynx LLC, assignee. Controlled Release from Macromolecular Conjugates. US patent US8754190B2. 2014.
17. Fontaine SD, Hann B, Reid R, Ashley GW, Santi DV. Species-specific optimization of PEG~SN-38 prodrug pharmacokinetics and antitumor effects in a triple-negative BRCA1-deficient xenograft. Cancer Chemother Pharmacol 2019; 84:729–38. [PubMed: 31321449]
18. Beckford Vera DR, Fontaine SD, VanBrocklin HF, Hearn BR, Reid R, Ashley GW, et al. PET imaging of the EPR effect in tumor xenografts using small 15 nm diameter polyethylene glycols labeled with zirconium-89. Mol Cancer Ther 2020; 19:673–9. [PubMed: 31744896]
19. Pommier Y, O'Connor MJ, de Bono J. Laying a trap to kill cancer cells: PARP inhibitors and their mechanisms of action. Sci Transl Med 2016;8:362ps17.
20. Murai J, Pommier Y. PARP trapping beyond homologous recombination and platinum sensitivity in cancers. Annu Rev Cancer Biol 2019;3:131–50.
21. Boussios S, Abson C, Moschetta M, Rassy E, Karathanasi A, Bhat T, et al. Poly (ADP-Ribose) polymerase inhibitors: talazoparib in ovarian cancer and beyond. Drugs R D 2020;20:55–73. [PubMed: 32215876]
22. de Bono J, Ramanathan RK, Mina L, Chugh R, Glaspy J, Rafii S, et al. Phase I, dose-escalation, two-part trial of the parp inhibitor talazoparib in patients with advanced germline BRCA1/2 mutations and selected sporadic cancers. Cancer Discov 2017;7:620–9. [PubMed: 28242752]
23. Joyce AP, Wang M, Lawrence-Henderson R, Filliettaz C, Leung SS, Xu X, et al. One mouse, one pharmacokinetic profile: quantitative whole blood serial sampling for biotherapeutics. Pharm Res 2014;31:1823–33. [PubMed: 24464271]
24. Schmidt KT, Peer CJ, Huitema ADR, Williams MD, Wroblewski S, Schellens JHM, et al. Measurement of NLG207 (formerly CRLX101) nanoparticle-bound and released camptothecin in human plasma. J Pharm Biomed Anal 2020;181: 113073.
25. Houghton PJ, Morton CL, Tucker C, Payne D, Favours E, Cole C, et al. The pediatric preclinical testing program: description of models and early testing results. Pediatr Blood Cancer 2007;49:928–40. [PubMed: 17066459]
26. Morton CL, Houghton PJ. Establishment of human tumor xenografts in immunodeficient mice. Nat Protoc 2007;2:247–50. [PubMed: 17406581]
27. Drean A, Williamson CT, Brough R, Brandsma I, Menon M, Konde A, et al. Modeling therapy resistance in BRCA1/2-mutant cancers. Mol Cancer Ther 2017;16:2022–34. [PubMed: 28619759]
28. Milletti F, Storchi L, Goracci L, Bendels S, Wagner B, Kansy M, et al. Extending pKa prediction accuracy: high-throughput pKa measurements to understand pKa modulation of new chemical series. Eur J Med Chem 2010;45:4270–9. [PubMed: 20633962]
29. Bagno A, Scorrano G, Terrier F. The excess basicity of alkali metal methoxides in methanol. J Chem Soc Perkin Trans 1990;2:1017–27.
30. Bundgaard H,Johansen M. Prodrugs as drug delivery systems. XIX. Bioreversible derivatization of aromatic amines by formation of N-Mannich bases with succinimide. Int J Pharm 1981;8:183–92.
31. Stewart E, Goshorn R, Bradley C, Griffiths LM, Benavente C, Twarog NR, et al. Targeting the DNA repair pathway in Ewing sarcoma. Cell Rep 2014;9:829–41. [PubMed: 25437539]
32. Smith MA, Reynolds CP, Kang MH, Kolb EA, Gorlick R, Carol H, et al. Synergistic activity of PARP inhibition by talazoparib (BMN 673) with temozolomide in pediatric cancer models in the pediatric preclinical testing program. Clin Cancer Res 2015;21:819–32. [PubMed: 25500058]
33. Smith MA, Hampton OA, Reynolds CP, Kang MH, Maris JM, Gorlick R, et al. Initial testing (stage 1) of the PARP inhibitor BMN 673 by the pediatric preclinical testing program: PALB2 mutation predicts exceptional in vivo response to BMN 673. Pediatr Blood Cancer 2015;62:91–8. [PubMed: 25263539]

34. Wang B, Chu D, Feng Y, Shen Y, Aoyagi-Scharber M, Post LE. Discovery and characterization of (8S,9R)-5-fluoro-8-(4-fluorophenyl)-9-(1-methyl-1h-1,2,4-triazol-5-yl)-2,7,8,9-te trahydro-3h-pyrido[4,3,2-de]phthalazin-3-one (BMN 673, Talazoparib), a novel, highly potent, and orally efficacious poly(ADP-ribose) polymerase-1/2 inhibitor, as an anticancer agent. J Med Chem 2016;59: 335–57. [PubMed: 26652717]
35. Finan B, Ma T, Ottaway N, Muller TD, Habegger KM, Heppner KM, et al. Unimolecular dual incretins maximize metabolic benefits in rodents, monkeys, and humans. Sci Transl Med 2013;5:209ra151.
36. Goldstein MJ, Peters M, Weber BL, Davis CB. Optimizing the therapeutic window of targeted drugs in oncology: potency-guided first-in-human studies. Clin Transl Sci 2020[Epub ahead of print].
37. Levasseur LM, Slocum HK, Rustum YM, Greco WR. Modeling of the time-dependency of in vitro drug cytotoxicity and resistance. Cancer Res 1998;58: 5749–61. [PubMed: 9865733]
38. Holm C, Covey JM, Kerrigan D, Pommier Y. Differential requirement of DNA replication for the cytotoxicity of DNA topoisomerase I and II inhibitors in Chinese hamster DC3F cells. Cancer Res 1989;49:6365–8. [PubMed: 2553254]
39. Herriott A, Tudhope SJ, Junge G, Rodrigues N, Patterson MJ, Woodhouse L, et al. PARP1 expression, activity and ex vivo sensitivity to the PARP inhibitor, talazoparib (BMN 673), in chronic lymphocytic leukaemia. Oncotarget 2015; 6:43978–91. [PubMed: 26539646]
40. Rottenberg S, Jaspers JE, Kersbergen A, van der Burg E, Nygren AO, Zander SA, et al. High sensitivity of BRCA1-deficient mammary tumors to the PARP inhibitor AZD2281 alone and in combination with platinum drugs. Proc Natl Acad Sci U S A 2008;105:17079–84. [PubMed: 18971340]
41. Zander SA, Sol W, Greenberger L, Zhang Y, van Tellingen O, Jonkers J, et al. EZN-2208 (PEG-SN38) overcomes ABCG2-mediated topotecan resistance in BRCA1-deficient mouse mammary tumors. PLoS One 2012;7:e45248.
42. Thomas A, Pommier Y. Targeting topoisomerase I in the Era of precision medicine. Clin Cancer Res 2019;25:6581–9. [PubMed: 31227499]
43. Houston ZH, Bunt J, Chen KS, Puttick S, Howard CB, Fletcher NL, et al. Understanding the uptake of nanomedicines at different stages of brain cancer using a modular nanocarrier platform and precision bispecific antibodies. ACS Cent Sci 2020;6:727–38. [PubMed: 32490189]
44. Adkins CE, Nounou MI, Hye T, Mohammad AS, Terrell-Hall T, Mohan NK, et al. NKTR-102 Efficacy versus irinotecan in a mouse model of brain metastases of breast cancer. BMC Cancer 2015;15:685. [PubMed: 26463521]

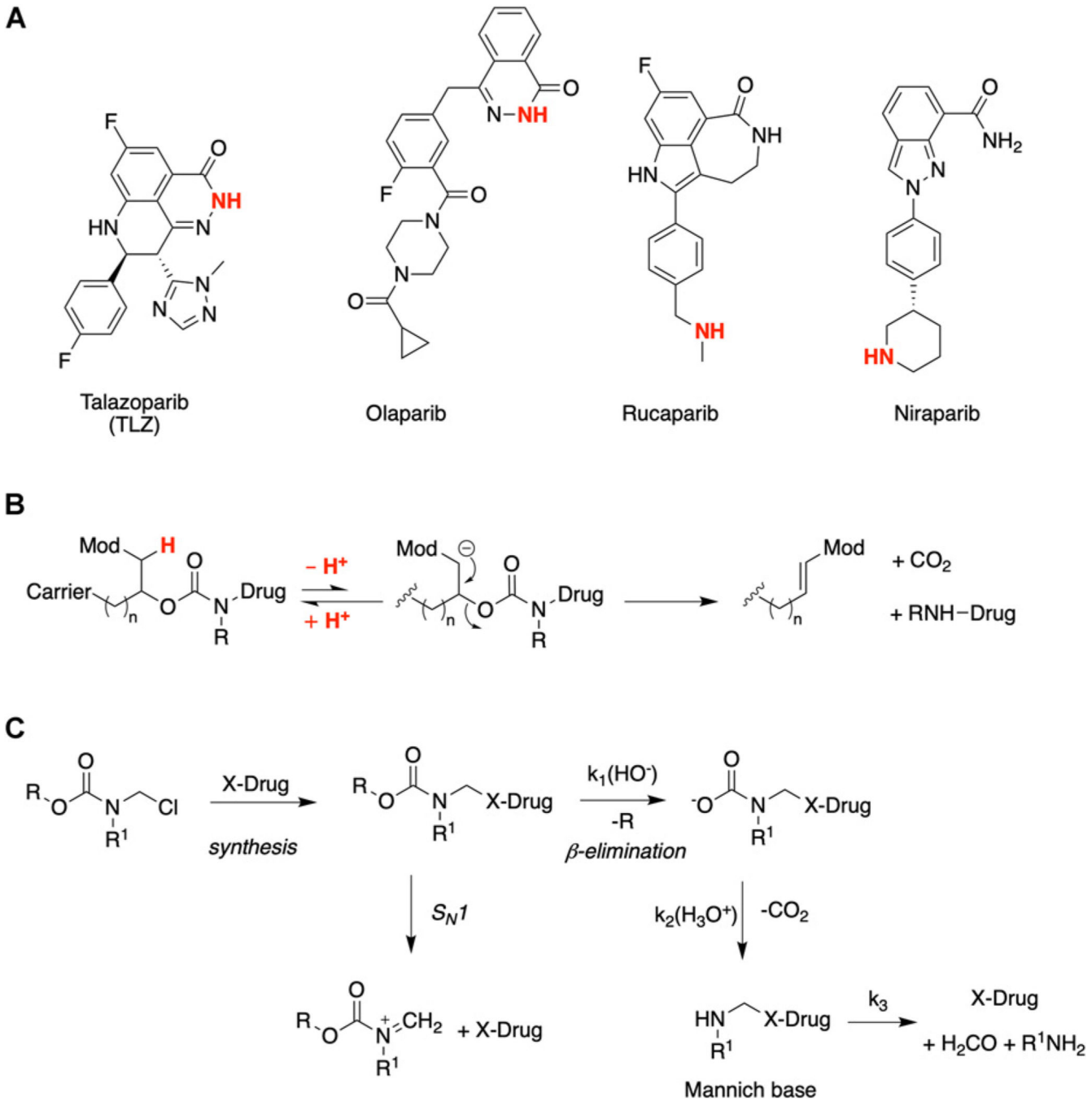

Figure 1.

A, Structures of the four approved PARPi. Heteroatoms compatible with covalent attachment to β-eliminative linkers are indicated in red. **B,** General mechanism for release of amine containing drugs mediated by β-elimination. **C,** Schematic showing the strategy for conjugation and mechanism of release of drugs containing poorly nucleophilic heteroatoms such as the phthalazinone of TLZ. Here, the R^1 group stabilizes the carbamate favoring the β-eliminative pathway over spontaneous S_N1-mediated release.

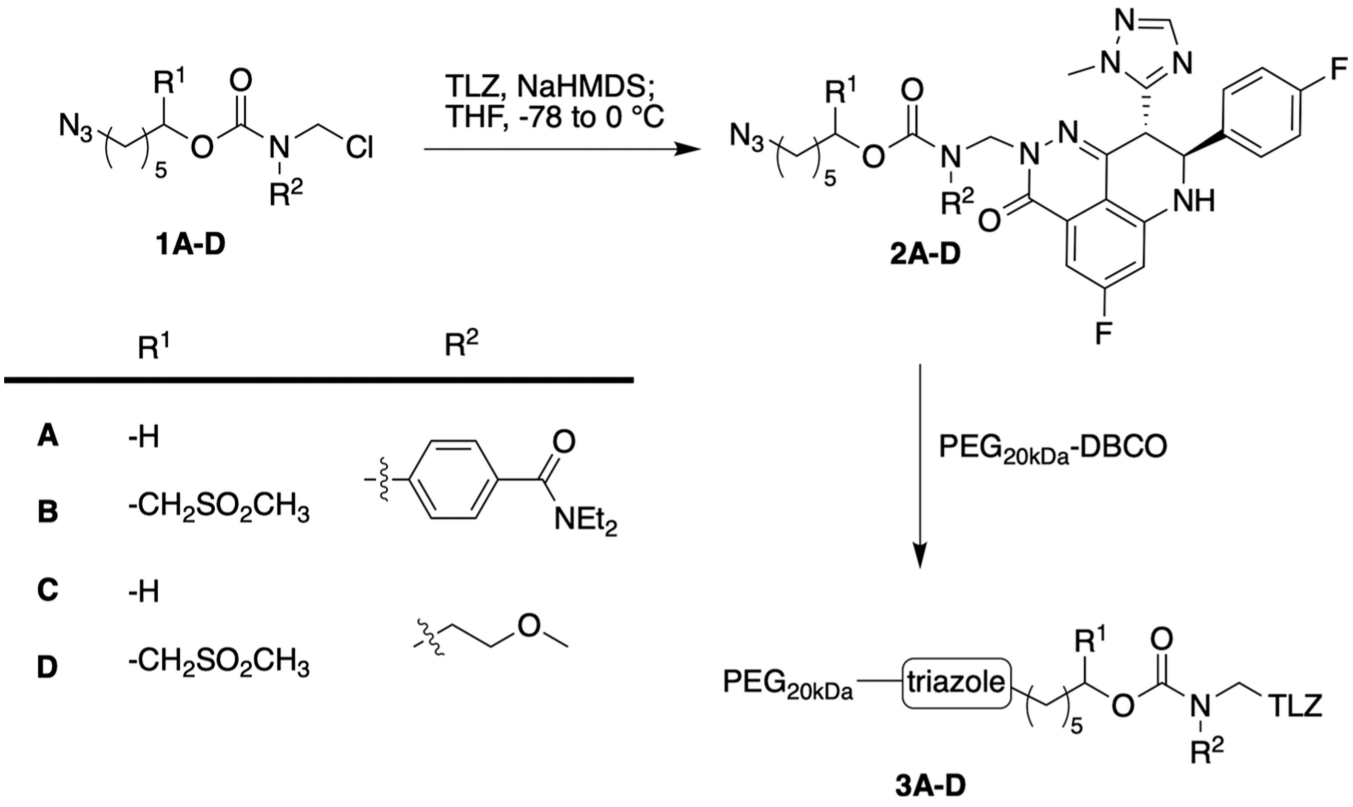

Figure 2.

Preparation of PEG_{20kDa}~TLZ conjugates **3A,B** bearing an N-aryl stabilizing group and **3C,D** bearing an N-alkyl stabilizing group.

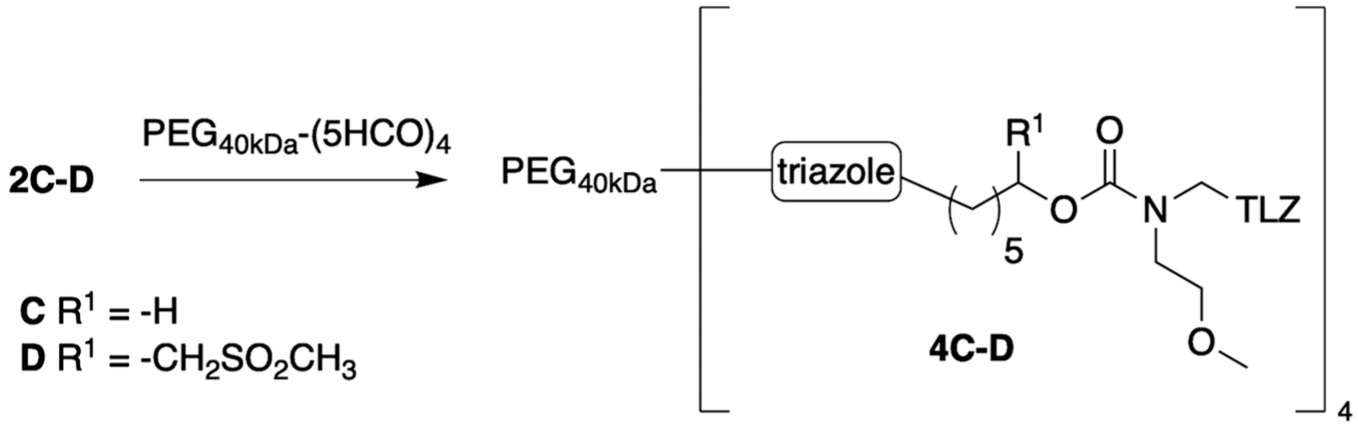

Figure 3.
Preparation of PEG_{40kDa}~$(TLZ)_4$ conjugates **4C** and **4D.**

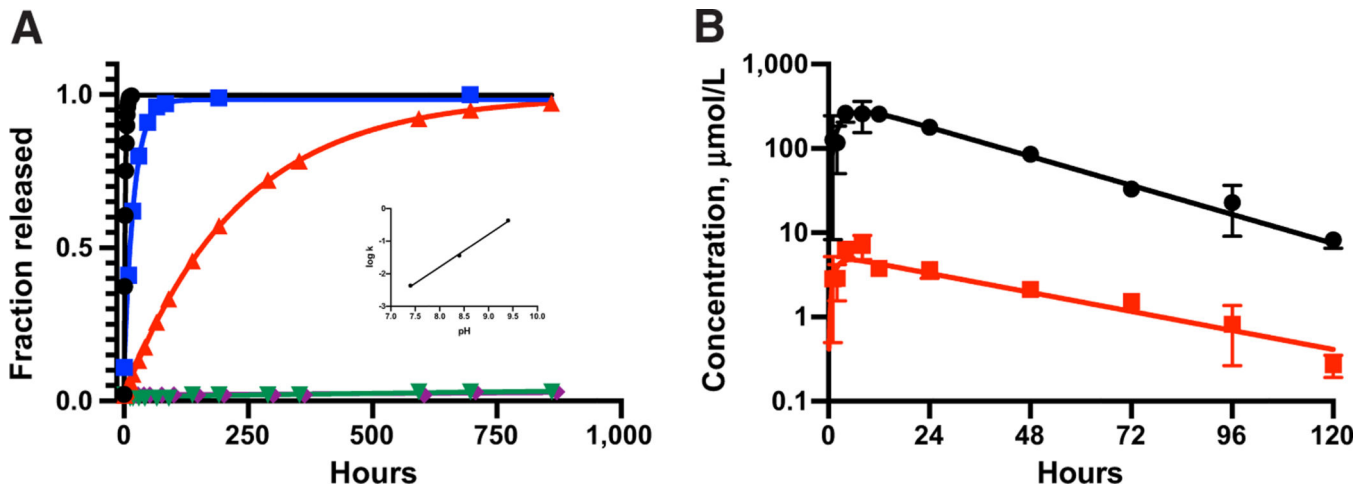

Figure 4.

In vitro and *in vivo* characterization of **4D. A,** *In vitro* release of TLZ from PEG_{40kDa}~$(TLZ)_4$ **4D** at pH 9.4 (●), pH 8.4 (■), pH 7.4 (▲), pH 5.0 (▼), and pH 1.1 (♦) at 37°C; inset is the pH-log k_{obsd} plot for TLZ release, $m = 1.00$, $R^2 = 0.998$. **B,** Plasma C vs. t plot for PEG–TLZ conjugate 4D (●) and released TLZ (■) after an intraperitoneal dose of 30 μmol/kg in mice. Data are mean ± SD.

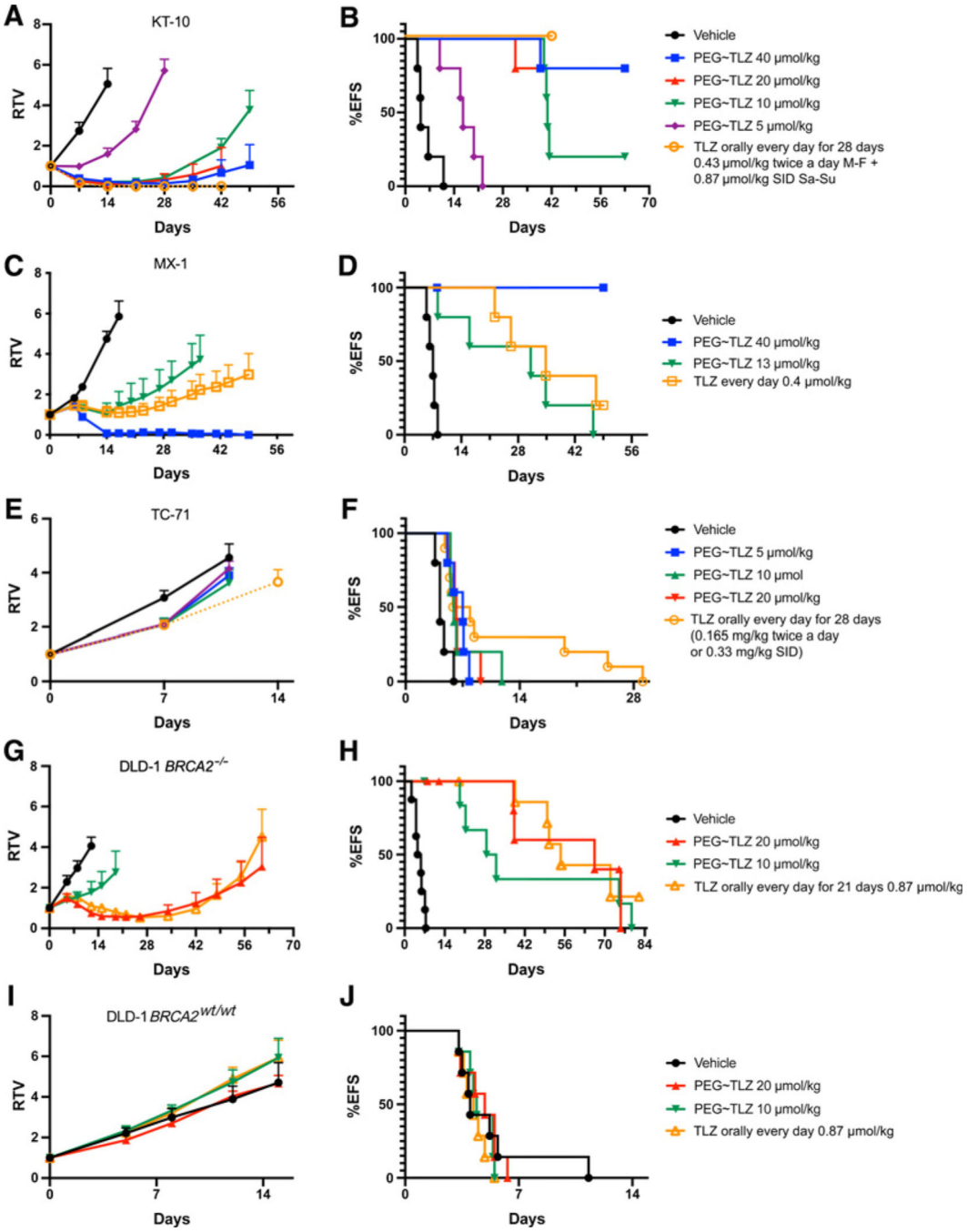

Figure 5.

Antitumor effects of PEG_{40kDa}~$(TLZ)_4$, **4D.** Response of KT-10 (**A** and **B**), MX-1 (**C** and **D**), TC-71 (**E** and **F**), DLD-1 *BRCA2*$^{-/-}$ (**G** and **H**), and DLD-1 *BRCA2*$^{wt/wt}$ (**I** and **J**) xenografts to **4D.** Relative tumor volume mean ± SEM vs. *t* (**A, C, E, G**, and **I**) and % EFS over study duration (**B, D, F, H,** and **J**), where an event is a two-fold increase in tumor volume from day 0. On *d* = 0, mice (*n* = 5 for **A, C,** and **E;** 8 for **G;** and 7 for **I**) received a single intraperitoneal dose of vehicle, or **4D** or every day doses of TLZ. In **D,** two mice treated with 40 μmol/kg **4D** were censored at *d* = 8 because of death, and the remaining

three did not reach event. Primary data in **A** and **E** for TLZ are from ref. 33. In **G,** three mice treated with **4D** at 20 μmol/kg died by day 14 and at 10 μmol/kg two mice died by day 19.

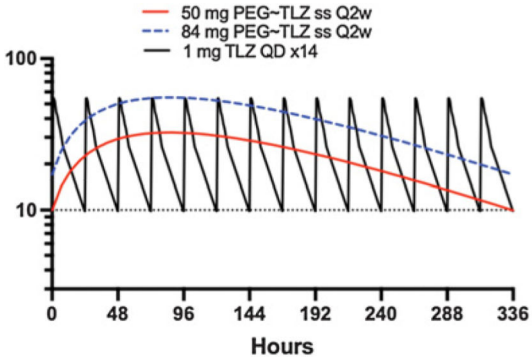

TLZ dose, human	$t_{1/2}$ (h)	C_{max} (nmol/L)	C_{min} (nmol/L)	C_{max}/C_{min}	AUC_{7d} (μmol/L*h)	AUC_{14d} (μmol/L*h)
TLZ 1 mg daily, ss	50	55	9.8	5.6	4.2	8.3
PEG~TLZ, 50 mg/every 2 weeks	288	32	10	3.2	NA	7.6
PEG~TLZ, 84 mg/every 2 weeks	288	53	17	3.2	NA	13

Figure 6.

Simulation of the pharmacokinetics of a PEG_{40kDa}~$(TLZ)_4$ with a release $t_{1/2}$ of 12 days in humans at steady state. *C* vs. *t* plots of simulated pharmacokinetic parameters of 1 mg every day TLZ (22) and TLZ released from every 2 weeks 50 mg (—) or 84 mg (- - -) PEG_{40kDa}~$(TLZ)_4$.

Table 1.

Pharmacokinetic parameters of PEG~TLZ **4D** and TLZ in the mouse.[a]

	TLZ, oral[b]		4D, intraperitoneal	TLZ from 4D
Dose, mmol/kg	0.87 every day[c]	0.66 twice a day[d]	30	
C_{max}	0.21	0.27	260 ± 28	7.0 ± 1.1
$t_{1/2,\alpha}$, hours	N/A	N/A	2.2 ± 0.4	N/A
$t_{1/2,\beta}$, hours	3	3	21 ± 1	32 ± 3
$t_{1/2,1}$, hours	N/A	N/A	200	N/A
$t_{1/2,2}$, hours			N/A	3.0[b]
$t_{1/2,3}$, hours	N/A	N/A	23[e]	N/A
AUC_{Wk}, μmol/L·h[f]	6.3	15	11,000	270

[a] Errors are ± SE.

[b] Calculated using data from ref. 31.

[c] Every day dose used here and in ref. 8.

[d] Reported MTD in tumor-free mice (32).

[e] Value based on $t_{1/2,\beta}$ of **4C** (Supplementary Fig. S9; Supplementary Table S3).

[f] On the basis of AUC_{0-24h} for PO TLZ and AUC_{0-120h} for **4D** and TLZ released from **4D.**